Effect of vertical mixing on the Atlantic Water layer circulation in the Arctic Ocean

Jinlun Zhang[1] and Mike Steele[1]

Received 25 May 2006; revised 29 September 2006; accepted 27 October 2006; published 13 March 2007.

[1] An ice-ocean model has been used to investigate the effect of vertical mixing on the circulation of the Atlantic Water layer (AL) in the Arctic Ocean. The motivation of this study comes from the disparate AL circulations in the various models that comprise the Arctic Ocean Model Intercomparison Project (AOMIP). It is found that varying vertical mixing significantly changes the ocean's stratification by altering the vertical distribution of salinity and hence the structure of the arctic halocline. In the Eurasian Basin, the changes in ocean stratification tend to change the strength and depth of the cyclonic AL circulation, but not the basic circulation pattern. In the Canada Basin, however, the changes in ocean stratification are sufficient to alter the direction of the AL circulation. Excessively strong vertical mixing drastically weakens the ocean stratification, leading to an anticyclonic circulation at all depths, including both the AL and the upper layer that consists of the surface mixed layer and the halocline. Overly weak vertical mixing makes the ocean unrealistically stratified, with a fresher and thinner upper layer than observations. This leads to an overly strong anticyclonic circulation in the upper layer and an overly shallow depth at which the underlying cyclonic circulation occurs. By allowing intermediate vertical mixing, the model does not significantly drift away from reality and is in a rather good agreement with observations of the vertical distribution of salinity throughout the Arctic Ocean. This realistic ocean stratification leads to a realistic cyclonic AL circulation in the Canada Basin. In order for arctic ice-ocean models to obtain realistic cyclonic AL circulation in the Canada Basin, it is essential to generate an upward concave-shaped halocline across the basin at certain depths, consistent with observations.

Citation: Zhang, J., and M. Steele (2007), Effect of vertical mixing on the Atlantic Water layer circulation in the Arctic Ocean, *J. Geophys. Res.*, *112*, C04S04, doi:10.1029/2006JC003732.

1. Introduction

[2] Significant changes in arctic climate have been detected in the past decades [*Hassol*, 2004]. There were observations of an increased presence of Atlantic Water in the Arctic Ocean in the 1990s [e.g., *McLaughlin et al.*, 1996; *Morison et al.*, 1998], owing to a strengthened Atlantic Water inflow through Fram Strait and the Barents Sea [e.g., *Grotefendt et al.*, 1998; *Zhang et al.*, 1998a; *Karcher et al.*, 2003]. Recent observations from the vicinity of the North Pole show that the Atlantic Water signature has lessened to near pre-1990s levels, although new warm pulses continue to enter the Arctic Ocean [*Polyakov et al.*, 2005]. Since the warm, saline Atlantic Water is an important source of heat and salt transport to the Arctic Ocean, the change and variability of its circulation impacts the polar climate system. For example, the increase in the Atlantic Water inflow in the 1990s is found to contribute to an increase in temperatures in various layers of the Arctic Ocean and a decline of arctic sea ice [*Zhang et al.*, 1998a, 2004].

[3] After entering the Arctic Ocean from Fram Strait and the Barents Sea, Atlantic Water is observed to dive under the fresher Arctic halocline (<200 m in depth) [*Steele and Boyd*, 1998] and flow as cyclonic boundary currents along shelves and ridges, with a few locations of cross-ridge flows [e.g., *Rudels et al.*, 1994; *Woodgate et al.*, 2001]. Atlantic Water spreads over the whole Arctic Ocean at the depths of 200–900 m often referred to as the Atlantic Water layer (AL). Above the AL is the upper layer (UL) that consists of a surface mixed layer and the halocline. One of the major goals of the Arctic Ocean Model Intercomparison Project (AOMIP) is to simulate and hence understand the behavior of the cyclonic AL circulation through coordinated numerical experiments involving more than ten coupled arctic ice-ocean models developed at various international institutions [*Proshutinsky et al.*, 2001, 2005]. However, these coordinated experiments have resulted in diverging results about the AL circulation pattern. As discussed by *Yang* [2005],

[1]Polar Science Center, Applied Physics Laboratory, College of Ocean and Fishery Sciences, University of Washington, Seattle, Washington, USA.

0148-0227/07/2006JC003732$09.00

only half of the AOMIP models participating in an earlier coordinated experiment were able to simulate an AL circulation pattern dominated by cyclonic flows, while the other half generated one dominated by anticyclonic flows (also see http://www.planetwater.ca/research/AOMIP/index.html). The lack of model consensus on the directions of the AL flows is also reported by *Holloway et al.* [2007] based on the latest AOMIP coordinated experiment.

[4] What causes the diverging model results? *Yang* [2005] found that a positive (negative) potential vorticity (PV) flux into the semi-enclosed Arctic Ocean through Fram Strait and the Barents Sea results in a cyclonic (anticyclonic) AL circulation in a barotropic ocean model. The importance of PV flux in shaping the AL circulation is also reflected by the study of M. J. Karcher et al. (On the dynamics of Atlantic Water circulation in the Arctic Ocean, submitted to *Journal of Geophysical Research*, 2007, hereinafter referred to as Karcher et al., submitted manuscript, 2007). Given that the Arctic Ocean is strongly stratified with the saltier AL underlying the fresher UL, are there any other ocean processes that may play a role in determining the AL circulation directions? Figures 4b and 7b from *Holloway et al.* [2007] show that the ocean stratification is intimately linked to the AL circulation. For example, the Alfred Wegener Institute (AWI) model has a cyclonic circulation from nearly the surface to the depth of about 800 m in the Canada Basin, in conjunction with a fresher and thinner UL than that simulated by most of the other models. In contrast, the Naval Postgraduate School model has an anticyclonic AL circulation in association with a less stratified upper ocean, similar to the result of *Zhang et al.* [1998a] using a rigid-lid ocean model (referred to as the UW-old model in Karcher et al. (submitted manuscript, 2007)).

[5] Does the apparent link between ocean stratification and AL circulation signal that the baroclinic component of the flows plays an important role in controlling the AL circulation directions? Ocean stratification is affected by a variety of ocean processes, but intuitively vertical mixing is likely to have a large impact. In this study, we focus on the effect of vertical mixing on the ocean's density structure and on the AL circulation. For this purpose, it is more effective to use a single ice-ocean model to conduct a series of numerical experiments with varying degrees of vertical mixing than to involve various AOMIP models with different model configurations and parameterizations. The ice-ocean model and the numerical experiments are described in section 2. The results are presented in section 3 and summarized in section 4.

2. Model Description

2.1. Coupled Ice-Ocean Model and AOMIP Forcing

[6] Referred to as the UW-new model in Karcher et al. (submitted manuscript, 2007), the coupled ice-ocean model consists of the Parallel Ocean Program (POP) developed at Los Alamos National Laboratory (LANL) and a sea ice model. The POP model is a *Bryan-Cox-Semtner* type ocean model [*Bryan*, 1969; *Cox*, 1984; *Semtner*, 1986] with numerous improvements, including an implicit free-surface formulation of the barotropic mode and model adaptation to parallel computing [e.g., *Smith et al.*, 1992; *Dukowicz and Smith*, 1994]. The sea ice model is based on *Zhang and*

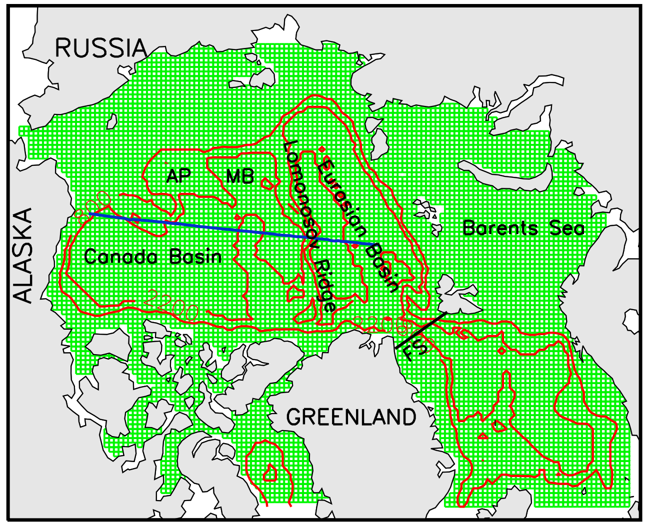

Figure 1. Model grid configuration (40-km horizontal resolution illustrated by green lines), and bathymetry (red contours with the interval being 1400 m). The blue line between Barrow, Alaska and a location in the Eurasian Basin represents part of the SCICEX cruise track in the fall of 2000 along which CTD measurements are available. Fram Strait (represented by the black line), Arlis Plateau, and Makarov Basin are marked as FS, AP, and MB.

Hibler [1997], which is also adapted to parallel computing [*Zhang and Rothrock*, 2003]. Embedded into the sea ice model is a snow model following *Zhang et al.* [1998b]. The coupled ice-ocean model is based on a generalized orthogonal curvilinear coordinate system, covering the Arctic Ocean, the Barents Sea, the GIN (Greenland-Iceland-Norwegian) Sea, and Baffin Bay, with a uniform horizontal resolution of 40 km (Figure 1). Vertically, the model has 25 ocean levels with various thicknesses.

[7] The POP ocean model is modified so that open boundary conditions can be specified along the model's lateral boundaries, including Bering Strait, Davis Strait, Denmark Strait, and Faroe-Shetland Passage. The open boundary conditions are obtained from a global coupled ice-ocean model, including monthly sea surface height and ocean velocity, temperature, and salinity over the period 1948–1978. Model initialization and atmospheric and riverine forcing follow the AOMIP protocols for the latest coordinated numerical experiment (see http://fish.cims.nyu.edu/project_aomip/overview.html and http://www.planetwater.ca/research/AOMIP/modelspecs.html), except that the initial condition is taken from *Levitus* [1982]. The atmospheric forcing includes daily NCAR/NCEP reanalysis sea level pressure (SLP) and surface air temperature; monthly precipitation climatology is from Serreze (personal communication), monthly cloudiness climatology from *Röske* [2001], and monthly river-runoff climatology from AWI [*Prange and Lohmann*, 2001] which is based on data from the Global River Data Center in Koblenz, Germany.

2.2. Design of Numerical Experiments With Vertical Mixing

[8] We want to examine the effect of vertical mixing on ocean stratification and the AL circulation by conducting a

series of numerical experiments with varying degrees of vertical mixing. Note that a number of vertical mixing schemes have been implemented in general ocean circulation models, including the traditional constant viscosity/diffusivity approach, the Richardson number-dependent scheme [*Pacanowski and Philander*, 1981], and the *Mellor and Yamada* [1982] turbulence closure scheme. We here choose the K-profile parameterization (KPP) scheme [*Large et al.*, 1994] used by LANL for most of our experiments. Mixing below the surface mixed layer is strongly influenced by a "background" diffusivity which we vary from a high value of 1.25 cm^2 s^{-1} (KPP1.25), a medium-high value of 0.25 cm^2 s^{-1} (KPP0.25), a medium-low value of 0.05 cm^2 s^{-1} (KPP0.05) and a low value of 0.01 cm^2 s^{-1} (KPP0.01). Background viscosity is always ten times the background diffusivity, in keeping with the procedure at LANL. An additional experiment with KPP turned off and only constant background diffusivity of 0.01 cm^2 s^{-1} (NoKPP0.01) is also employed to show results for very weak mixing. In order to single out the effect of vertical mixing, other model parameters are kept the same in all experiments, such as the horizontal viscosity coefficient (1.2×10^8 cm^2 s^{-1}) and diffusivity coefficient (4.0×10^5 cm^2 s^{-1}). Static instability in these simulations is treated by increasing the vertical viscosity and diffusivity coefficients to 500 cm^2 s^{-1}.

[9] Each experiment is a model simulation from 1948 to 1978. Following AOMIP protocols, the model surface salinity in these simulations is restored (with a restoring constant of 180 days) to the Polar Science Center Hydrographic Climatology (PHC [*Steele et al.*, 2001a, 2001b]) data for the first 11 years (1948–1958) of the integration. After 1958 no climate restoring is allowed and the model evolves freely to 1978. Unless stated otherwise, the 1978 mean results from various cases are presented and compared with the PHC climatology, which is based on the Environment Working Group [*EWG*, 1997, 1998] data for the Arctic, and the Submarine Science Expedition (SCICEX) measurements in fall of 2000.

3. Results

3.1. Effect of Vertical Mixing on Ocean Stratification

[10] In the Arctic Ocean density stratification is mainly controlled by the salinity distribution, and hence the pycnocline is often coincident with the halocline [*Steele and Boyd*, 1998]. Along the cruise track of SCICEX 2000 (Figure 1), the observations (both the PHC climatology and SCICEX measurements) of vertical salinity distribution show a fresh and shallow UL overlying the salty AL (Figures 2a and 2b). The halocline is significantly lower in the Canada Basin than in the Eurasian Basin. This is because the surface stress resulting from anticyclonic wind/ice forcing in the Canada Basin draws surface fresh water to the central Canada Basin via Ekman convergence, depressing the halocline through Ekman pumping [*Proshutinsky et al.*, 2002]. Westward winds along the shelf break are also favorable for upwelling [*Pickart*, 2004], an effect reflected in the SCICEX data since the salinity contours bend toward the surface near the Alaska coast (Figure 2b) The upwelling effect is smoothed or not resolved in the PHC climatology since its salinity contours stay quite flat near the coast (Figure 2a).

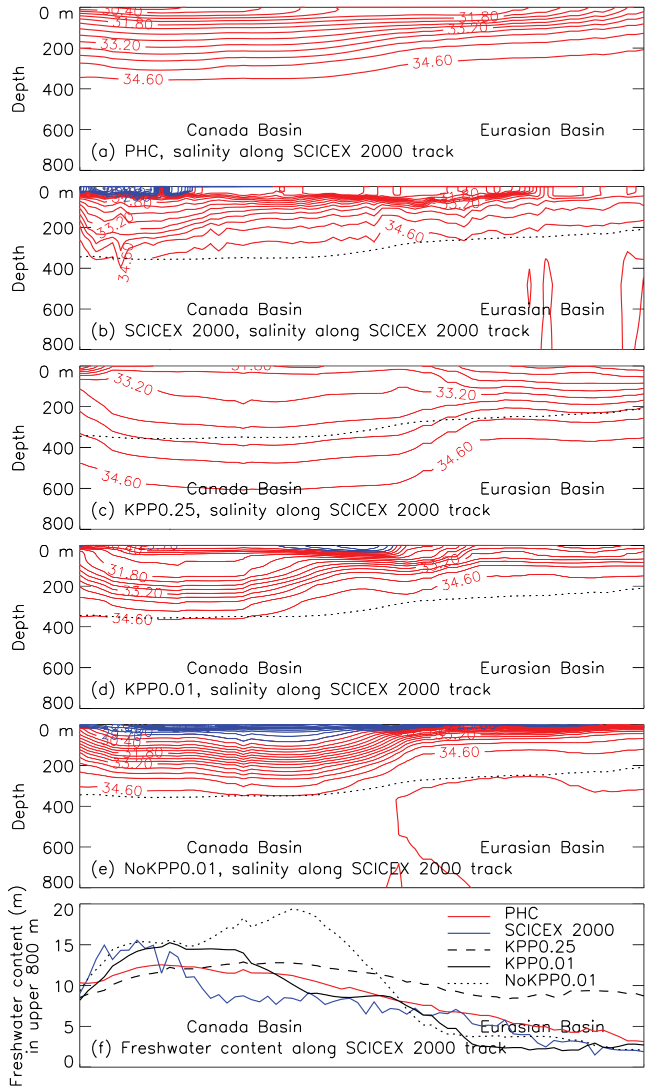

Figure 2. The 1978 mean vertical distribution of salinity (a–e) and freshwater (FW) content integrated in the upper 800 m (f) along the cruise track of SCICEX 2000. Reference salinity of 34.8 psu is used to calculate the FW content. Blue (red) contours in (b–e) represent salinity below (above) 30.00 psu with contour interval 0.35 psu. The dotted line in (b–e) is the 34.60 psu contour from (a).

[11] In the KPP0.25 case with relatively strong vertical mixing, the simulated salinity at the surface and in the UL is larger than observations throughout the Canada and Eurasian basins (Figure 2c). The simulated 34.6 psu salinity contour is about 100 m deeper than observations in the Eurasian Basin and more than 200 m deeper in the Canada Basin, a substantial model bias in ocean stratification. This result shows that strong vertical mixing in the Canada Basin, combined with Ekman pumping, tends to greatly depress the halocline, thus weakening the stratification of the ocean. Even in the Eurasian Basin where Ekman pumping is unlikely owing to cyclonic surface stress, strong vertical mixing still spreads the halocline over a greater depth range.

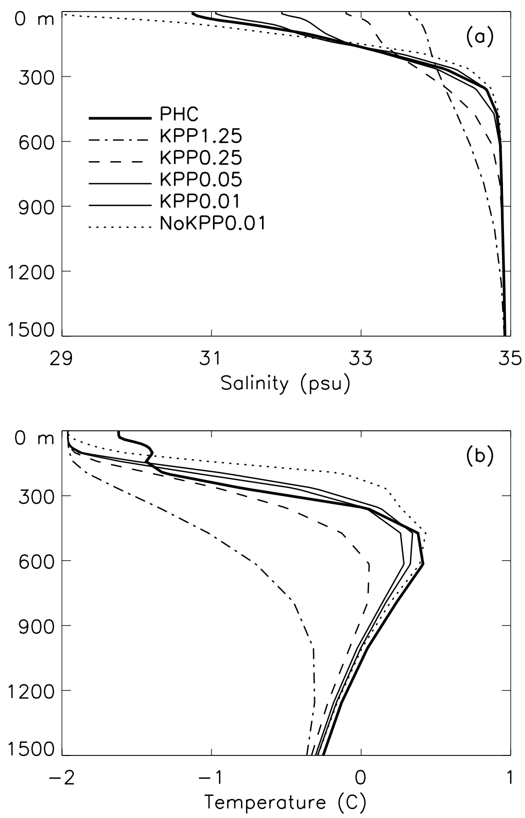

Figure 3. The 1978 mean vertical profiles of salinity and temperature averaged over the Canada Basin.

[12] In contrast, the vertical salinity distribution simulated by the KPP0.01 experiment is in good agreement with the observations in both the Canada and Eurasian basins (Figure 2d). Both surface and deeper salinities are the closest of all experiments to the PHC and SCICEX data. In addition, the simulated salinity contours also bend toward the surface near the Alaska coast, suggesting that the model is able to simulate upwelling in that area.

[13] The case of very weak vertical mixing NoKPP0.01 generates much fresher water in the UL than observations throughout the Canada and Eurasian basins (Figure 2e), and a shallower halocline. Reducing mixing below this value has little additional effect. In the opposite extreme, the case of very strong vertical mixing (KPP1.25) generated results so far away from observation that they are not included in Figure 2. However, KPP1.25 is included in Figure 3, which compares salinity and temperature profiles averaged over the Canada Basin. As can be seen, weak vertical mixing tends to create a sharper halocline, while strong mixing has the opposite effect (Figure 3a). The excessive mixing allowed in KPP1.25 nearly destroys the halocline. The salinity profile generated by KPP0.01 has the best match with PHC climatology in the whole water column (Figure 3a).

[14] The simulated surface temperature is the same for all experiments and is lower than the PHC climatology (Figure 3b). This is because the freezing point of sea water is set to be constant ($-1.96°C$) in the model. Halocline temperatures simulated by KPP0.05 and KPP0.01 are close to observations, while those simulated by NoKPP0.01 are warmer than observations, likely owing to inadequate vertical mixing in the UL. As expected, stronger vertical mixing (KPP1.25 and KPP0.25) causes more heat to escape from the AL to the surface so that the AL temperature is significantly lower than observations. Weaker mixing, on the other hand, is able to keep the AL temperature close to observations, which indicate that the simulated heat transport from the AL to the surface may be more realistic.

3.2. Effect of Vertical Mixing on Freshwater Distribution

[15] The vertically integrated freshwater (FW) distribution is closely linked to the upper ocean salinity distribution and therefore expected to be similarly affected by vertical mixing. The PHC data indicate high FW values in the Canada Basin and low in the Eurasian Basin (Figure 4d). In the NoKPP0.01 case with weak vertical mixing, the simulated FW content in the Canada and Makarov basins is considerably greater than those simulated by KPP0.01 and KPP0.25, while that in the Eurasian Basin is smaller. This is because strong background mixing forces FW down below the Ekman convergence layer of the Canada and Makarov Basins, while weak mixing keeps more of the FW in the Ekman convergence layer. The mean 1978 convergence of freshwater $-\nabla \bullet (u \times FW)$ in KPP1.25 is about half that in NoKPP0.01 within the upper 20 m of the Canada Basin. Along the cruise track of SCICEX 2000, the FW content of KPP0.01 and KPP0.05 (not shown) is in a generally better agreement with the PHC/SCICEX data than other cases (Figure 2f), although differences remain. Note that the spatial pattern of sea surface height (SSH, not shown) is almost identical to that of FW content, indicating that SSH is highly correlated to FW content in the Arctic Ocean [e.g., *Steele and Ermold*, 2007].

3.3. Effect of Vertical Mixing on Atlantic Layer Circulation

[16] So far, the experiments have demonstrated that varying vertical mixing profoundly impacts the simulation of the Arctic Ocean's salinity/temperature structure, stratification, SSH, and FW content. Does vertical mixing also affect the AL circulation? It appears that the impact has already manifested itself even before Atlantic Water enters the Arctic Ocean. At Fram Strait, one of the two Atlantic Water entrances into the Arctic, the vertical distribution of horizontal velocity is different among the experiments (Figure 5). These experiments all show that AL flows into the Arctic Ocean mainly at the east side of the strait and the arctic water flows out at the west side. However, strong vertical mixing (KPP0.25) tends to deepen the AL and weaken both Atlantic Water inflow and arctic water outflow in the surface layer, whereas the cases of weak (NoKPP0.01) and intermediate (KPP0.01) vertical mixing tend to strengthen the outflow below the AL. The weak mixing case of NoKPP0.01 also has a weaker Atlantic Water inflow at Fram Strait than the cases of KPP0.05 and KPP0.01 (Figure 5).

[17] After flowing through Fram Strait and the Barents Sea, modeled Atlantic Water enters the Eurasian Basin and flows generally in a cyclonic direction along the rim of the Eurasian Basin; some also crosses the Lomonosov Ridge into the Makarov and Canada basins at various latitudes

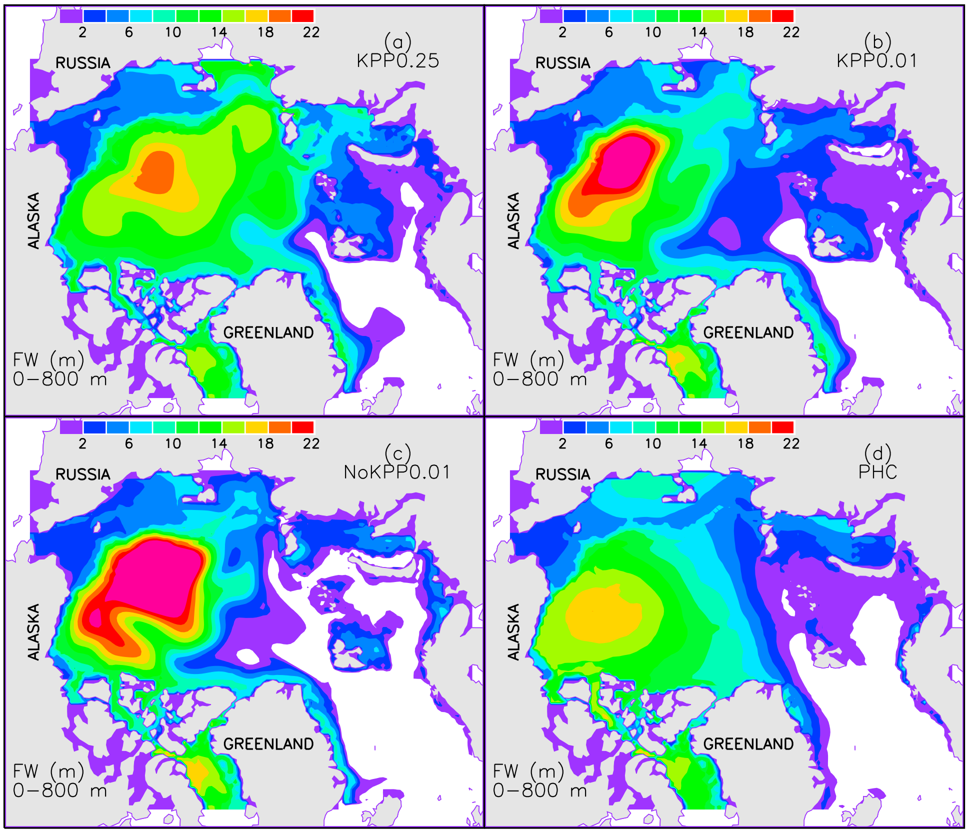

Figure 4. (a–c) The 1978 mean freshwater (FW) content integrated in the upper 800 m. (d) Same for 1950–1990 mean conditions in the PHC database.

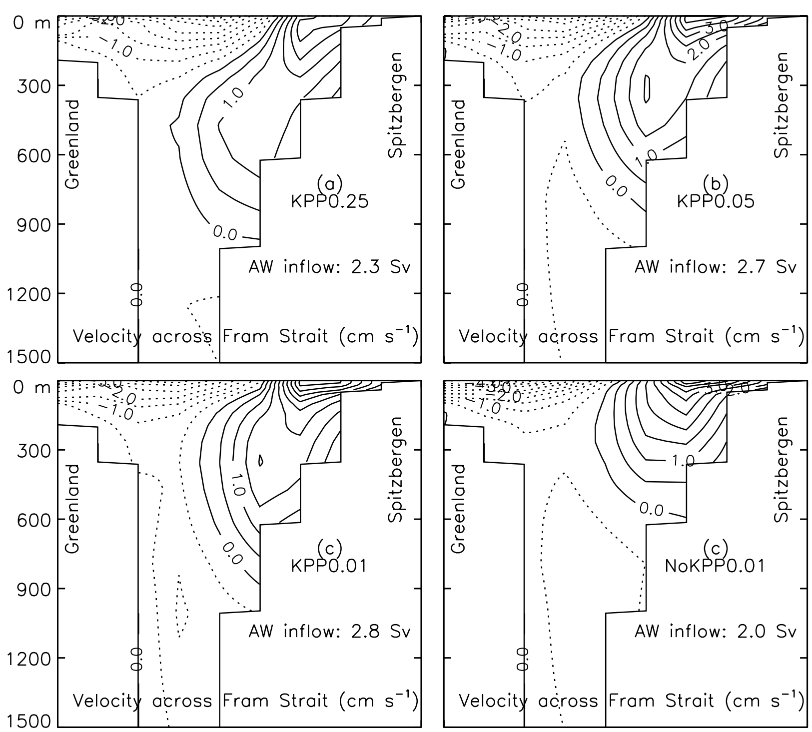

Figure 5. The 1978 mean vertical distribution of horizontal velocity across Fram Strait (see the black line in Figure 1). Solid lines represent Atlantic water inflow to the Arctic, dashed lines out of the Arctic. Also shown are the values of total Atlantic water inflow at Fram Strait.

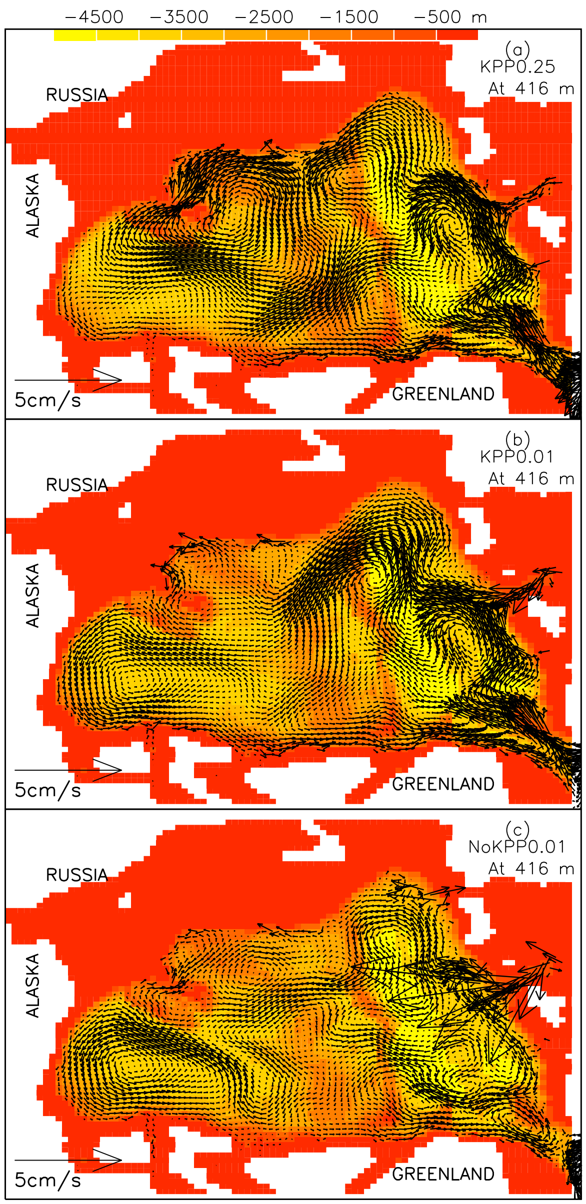

Figure 6. The 1978 mean ocean velocity at 416 m depth (ocean level 13). Model bathymetry is shown by color contours.

(Figure 6). At the depth of 416 m, the 3 main experiments differ in the strength of the AL flows. However, the basic pattern of the cyclonic AL circulation in the Eurasian Basin is similar among the experiments, even though the generated halocline structure is significantly different (Figure 2). This is not the case in the Makarov and Canada Basins. Strong vertical mixing case KPP0.25 creates a more vigorous anticyclonic circulation in the Arlis Plateau and Makarov Basin, with a weak cyclonic circulation in the Canada Basin. With reduced mixing, both KPP0.01 and NoKPP0.01 obtain a well defined cyclonic AL circulation in the Canada Basin; the anticyclonic circulation in the Arlis Plateau and Makarov Basin is considerably weaker than that simulated by KPP0.25.

[18] The effect of vertical mixing on the AL circulation is further illustrated by Figure 7, which compares profiles of normalized topostrophy integrated for the Canada Basin. A detailed definition of topostrophy is given in *Holloway et al.* [2007]. Briefly, topostrophy is a scalar given by the upwards component of $\mathbf{V} \times \nabla D$, where $\mathbf{V}$ is velocity and ∇D is the gradient of total depth. In the northern hemisphere, flow with shallower water to the right (left) is characterized by positive (negative) topostrophy. Therefore in the Arctic Ocean, strongly positive (negative) topostrophy corresponds to flows dominated by cyclonic (anticyclonic) circulation along steep topography.

[19] As can be seen in Figure 7, NoKPP0.01 generates the strongest anticyclonic circulation at the surface, with cyclonic AL circulation starting at about 130 m (level of no motion), and peaking at about 200 m depth. KPP0.01 starts and peaks its cyclonic AL circulation at about the same depths as NoKPP0.01. With strong vertical mixing, KPP0.25 starts its cyclonic AL circulation at a depth of about 350 m, indicating that increased vertical mixing not only depresses the pycnocline, but also extends the anticyclonic circulation deeper. When the mixing becomes outright excessive (KPP1.25) based on its performance, the halocline is essentially destroyed (Figure 3), and the cyclonic circulation vanishes at most depths.

[20] Like topostrophy, vorticity is also useful to measure the direction and intensity of the rotation of the arctic waters. The vorticity averaged over the whole water column of the Arctic Basin is negative for all the experiments (Table 1) owing to the UL anticyclonic circulation. However, the vorticity increases with decreasing vertical mixing. This is because the vorticity averaged over the water column below 200 m increases with decreasing vertical mixing, indicating strengthened cyclonic AL circulation, as also shown in Figure 7.

[21] The studies of *Yang* [2005] and Karcher et al. (submitted manuscript, 2007) demonstrated the link between the PV flux into the Arctic Basin and the pattern of AL circulation. Particularly, *Yang* [2005], using a barotropic ocean model, found that a positive PV flux into the Arctic Basin results in a cyclonic AL circulation in both the Canada Basin and Eurasian Basin, while a negative PV flux results in an anticyclonic AL circulation in these basins. Karcher et al. (submitted manuscript, 2007) noted that for the subsurface

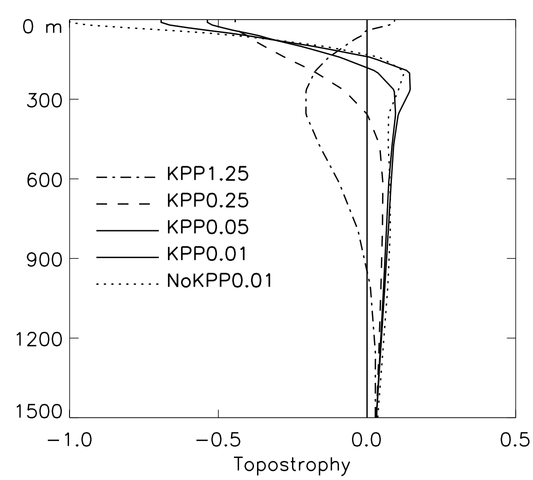

Figure 7. The 1978 mean normalized topostrophy integrated over the Canada Basin.

Table 1. The 1978 Mean Vorticities (% yr^{-1}) Integrated in the Whole and Part (Below 200 m) of the Water Column of the Arctic Basin and 1978 Mean Potential Vorticity (PV) Fluxes (m^2 s^{-2}) Into the Arctic Basin Through Various Atlantic Water Passages

	KPP1.25	KPP0.25	KPP0.05	KPP0.01	NoKPP0.01
Vorticity of the whole basin	−3.6	−2.1	−1.6	−1.4	−0.6
Vorticity below 200 m	−0.11	0.13	0.16	0.21	0.20
PV flux (St. Anna Trough)	−0.18	0.16	0.34	0.28	0.69
PV flux (Fram Strait)	−0.23	−0.02	−0.02	−0.01	−0.23
PV flux (St. Anna Tr. + Fram St.)	−0.41	0.14	0.32	0.27	0.46

AL circulation, it is only the fluxes through the relatively deep channels of Fram Strait and the Barents Sea that influence Arctic Ocean circulation. Table 1 shows these fluxes. The greatest inflow from the Barents Sea into the Arctic Ocean occurs between Franz Josef Land and Severnaya Zemlya in the St. Anna Trough. The PV flux through this channel is generally larger than that through the less-stratified Fram Strait. The total PV flux through both channels is related to the vorticity and topostrophy of the Arctic Ocean AL in the manner described by *Yang* [2005]; i.e., negative (positive) vorticity/topostrophy is linked to negative (positive) PV inflow. These PV fluxes change in response to changes both within the Arctic Ocean and in the larger domain as well.

3.4. Effect of Vertical Mixing on Model Drift

[22] Arctic ice-ocean models are often subject to significant model drift [*Zhang et al.*, 1998b; *Steele et al.*, 2001a, 2001b]. This is because there are many uncertainties in the models' representations of physical processes, including the parameterization of mixing. Does and to what degree vertical mixing affect the drift of arctic ice-ocean models? With strong vertical mixing (KPP1.25), the simulated ocean loses both heat and salt rapidly and the model drifts away from the temperature and salinity climatology (initial conditions) faster than any of other experiments (Figures 8a and 8b). With weak mixing (NoKPP0.01), the heat is trapped in the ocean and the ocean becomes much warmer than the climatology and other cases. In the cases of KPP0.01 and KPP0.05, the model drift in temperature and salinity is relatively small.

[23] Figure 8c shows the evolution of the vorticity averaged over the water column below 200 m in the Arctic Basin. Since the model starts with zero velocity, the average vorticity is close to zero initially. The model's climate restoring to PHC climatology from 1948 to 1958 tends to create positive vorticity below 200 m, thus creating cyclonic AL circulation. After the restoring is removed from 1959, the strong mixing case (KPP1.25) drifts quickly such that an anticyclonic AL circulation forms. Other cases are able to maintain a cyclonic AL circulation, with less drift. However, weaker vertical mixing generally result in a greater positive vorticity and hence a stronger cyclonic AL circulation.

3.5. Explanation of How Vertical Mixing Affects the Atlantic Layer Circulation

[24] Figure 9 aims at explaining why varying vertical mixing impacts the AL circulation directions in the Canada Basin by altering the ocean's halocline/pycnocline. For this purpose, the density structure in the Canada Basin is idealized as a 2-layer fluid with fresher water in the UL and saltier water in the AL, assuming the halocline is infinitely sharp. This system is forced by surface stress due to anticyclonic wind/ice motion. The resulting Ekman transport causes freshwater water to converge in the UL and SSH to rise in the central Canada Basin (or the center of the anticyclonic gyre). It also causes the interface to rise at the

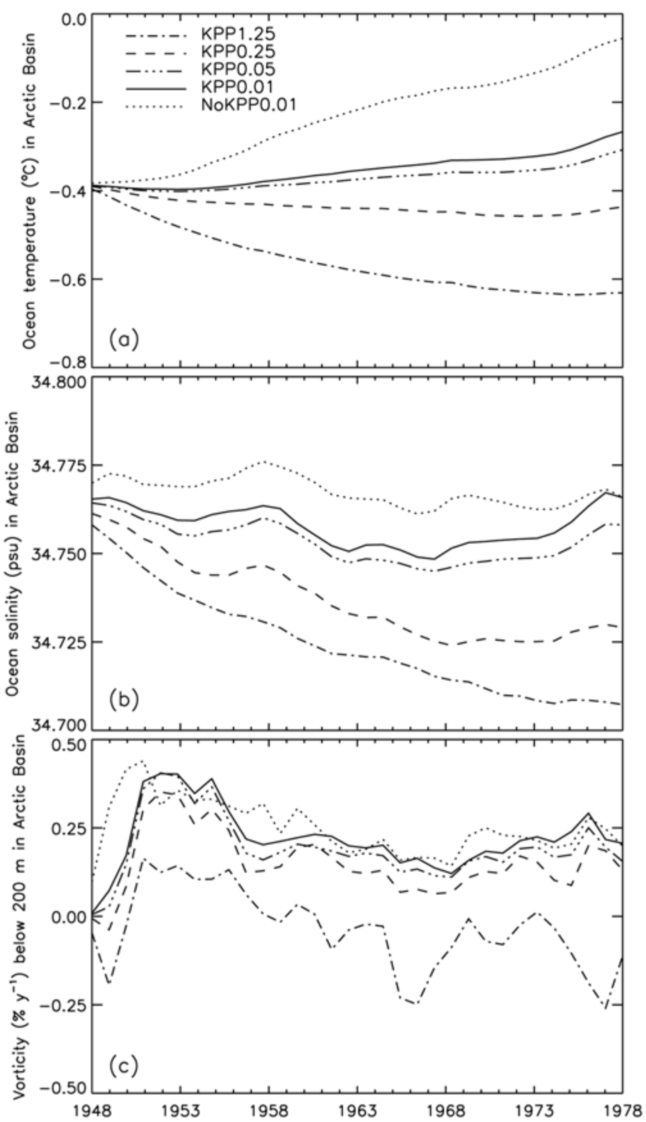

Figure 8. Evolution of annual mean ocean temperature, salinity, and vorticity.

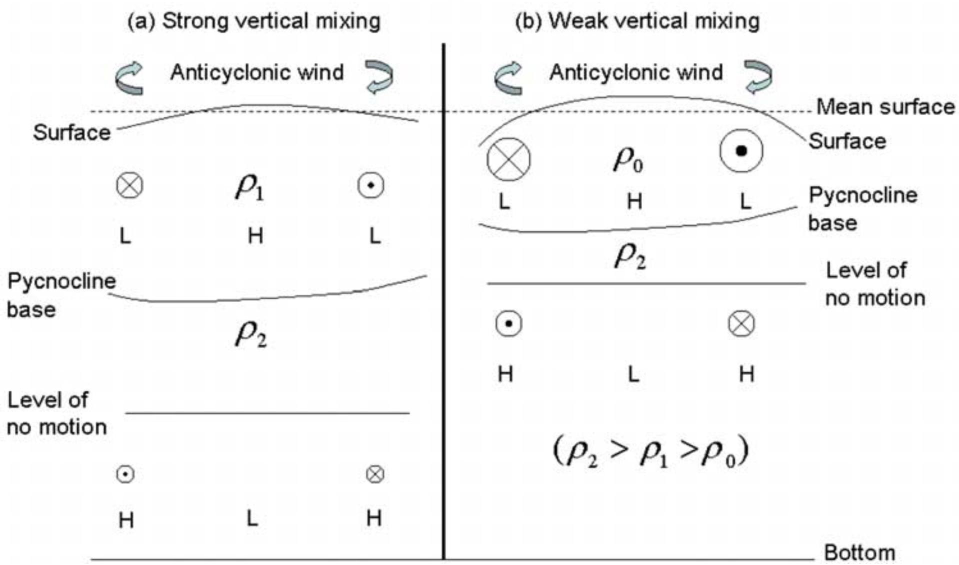

Figure 9. Illustration of the effect of varying vertical mixing on the AL circulation in the Canada Basin. The density (ρ) structure in the Canada Basin is simplified as a two-layer fluid with fresher water in the UL and saltier water in the AL. The circles with a cross represent geostrophic velocities into the page and circles with a dot represent flows out of the page. Letter L (H) represents low (high) pressure. The surface and pycnocline base are tilted slightly upward to the right, i.e., toward the Eurasian Basin.

perimeter of the basin where upwelling occurs [e.g., *Pickart*, 2004; *Carmack and Chapman*, 2003].

[25] With weaker vertical mixing, however, the UL is fresher and thinner because less salty AL water is entrained. Thus the Ekman layer converges more freshwater than when mixing is strong, resulting in a dome-shaped SSH (Figure 4) with higher pressure in the center and lower pressure at the perimeter. Such a spatial pressure pattern contributes to the maintenance of the anticyclonic circulation in the UL according to geostrophy.

[26] In contrast to the dome-shaped SSH, the halocline base in the Canada Basin is concave upwards (Figure 2), owing to upwelling at the shelf break. At some level in the AL, this concave-shaped halocline induces higher pressure at the perimeter of the Canada Basin and lower pressure at the center, because the AL density is higher than the UL density. Below that level (a level of no motion), the circulation is dominated by cyclonic geostrophic currents. In the case of weaker vertical mixing, the level of no motion is higher than the case of stronger mixing because of a shallower halocline and a greater density difference between the two layers (Figures 2 and 9). If vertical mixing is excessively weak (i.e., case NoKPP0.01), the anticyclonic circulation may be limited to an overly thin and fresh surface layer with cyclonic circulation below, an experiment that approaches the barotropic, no-wind experiments of *Yang* [2005]. In the case of excessively strong mixing (case KPP1.25), on the other hand, the anticyclonic circulation extends all the way to the bottom, without a sharp halocline (Figures 3 and 7).

4. Summary

[27] An AOMIP ice-ocean model has been used to investigate the effect of vertical mixing on the AL circulation of the Arctic Ocean. A series of model experiments have been conducted with varying degrees of vertical mixing. These experiments show that varying vertical mixing profoundly affects the ocean's stratification by altering the vertical distribution of salinity and hence the structure of the halocline. The changes in ocean stratification in turn determine the AL circulation pattern, particularly the sign of the circulation in the Canada Basin. If vertical mixing is too weak, the simulated ocean stratification is too strong, leading to a much warmer ocean temperature and an overly strong surface anticyclonic circulation under which cyclonic flow occurs. If vertical mixing is too strong, the ocean drifts rapidly away from reality and its stratification is drastically weakened, leading to an anticyclonic circulation in the Canada Basin that occurs at all depths, including both the UL and the AL. We find (for our model) an optimal value of background vertical diffusivity of 0.01 cm^2 s^{-1} while using the KPP scheme, and background viscosity of 0.1 cm^2 s^{-1}.

[28] These optimal values are probably unique to our particular model configuration and forcing. The main point we wish to make here is simply that vertical mixing schemes in numerical ice-ocean models can have a profound effect on the ocean circulation. Specifically, we have found that the amount of vertical mixing below the surface mixed layer can change the sign of AL circulation in the Canada and Makarov Basins of the Arctic Ocean. This happens via interplay between the fresh UL and the saltier AL below. The mixing also affects the stratification and thus the PV of the inflowing waters, which requires by PV conservation changes in the interior circulation.

[29] **Acknowledgments.** This research is supported by NSF Office of Polar Programs under Cooperative Agreements OPP-0002239 and OPP-0327664 with the International Arctic Research Center, University of Alaska Fairbanks. The model development is also supported by NSF grants OPP-0240916 and OPP-0229429, and NASA grants NNG04GB03G and NNG04GH52G. We thank A. Schweiger and M. Ortmeyer for computer assistance, and two anonymous reviewers for constructive comments.

References

Bryan, K. (1969), A numerical method for the study of the circulation of the world oceans, *J. Comput. Phys.*, *4*, 347–376.

Carmack, E., and D. C. Chapman (2003), Wind-driven shelf/basin exchange on an Arctic shelf: The joint roles of ice cover extent and shelf-break bathymetry, *Geophys. Res. Lett.*, *30*(14), 1778, doi:10.1029/2003GL017526.

Cox, M. D. (1984), A primitive equation, three-dimensional model of the oceans, *GFDL Ocean Group Tech. Rep. 1*, Geophys. Fluid Dyn. Lab., Natl. Oceanic and Atmos. Admin., Princeton Univ., Princeton, N. J.

Dukowicz, J. K., and R. D. Smith (1994), Implicit free-surface method for the Bryan-Cox-Semtner ocean model, *J. Geophys. Res.*, *99*, 7791–8014.

Environment Working Group (EWG) (1997), *Joint U.S.-Russian Atlas of the Arctic Ocean for the Winter Period* [CD-ROM], Natl. Snow and Ice Data Cent., Boulder, Colo.

Environment Working Group (EWG) (1998), *Joint U.S.-Russian Atlas of the Arctic Ocean for the Summer Period* [CD-ROM], Natl. Snow and Ice Data Cent., Boulder, Colo.

Grotefendt, K., K. Logemann, D. Quadfasel, and S. Ronski (1998), Is the Arctic Ocean warming?, *J. Geophys. Res.*, *103*, 27,679–27,687.

Hassol, S. J. (2004), *Impacts of a Warming Arctic: Arctic Climate Impact Assessment (ACIA)*, 139 pp., Cambridge Univ. Press, New York.

Holloway, G., et al. (2007), Water properties and circulation in Arctic Ocean models, *J. Geophys. Res.*, doi:10.1029/2006JC003642, in press.

Karcher, M. J., R. Gerdes, F. Kauker, and C. Koberle (2003), Arctic warming – Evolution and spreading of the 1990s warm event in the Nordic Seas and the Arctic Ocean, *J. Geophys. Res.*, *108*(C2), 3034, doi:10.1029/2001JC001265.

Large, W. G., J. C. McWilliams, and S. C. Doney (1994), Oceanic vertical mixing: A review and a model with a nonlocal boundary layer parameterization, *Rev. Geophys.*, *32*, 363–403.

Levitus, S. (1982), Climatological Atlas of the World Ocean, *NOAA Prof. Pap. 13*, 173 pp., U. S. Govt. Print. Off., Washington, D. C.

McLaughlin, F. A., E. C. Carmack, R. W. Macdonald, and J. K. B. Bishop (1996), Physical and geochemical properties across the Atlantic/Pacific water mass front in the southern Canadian Basin, *J. Geophys. Res.*, *101*, 1183–1197.

Mellor, G. L., and T. Yamada (1982), Development of a turbulence closure model for geophysical fluid problems, *Rev. Geophys.*, *20*, 851–865.

Morison, J. H., M. Steele, and R. Anderson (1998), Hydrography of the upper Arctic Ocean measured from the nuclear submarine USS Pargo, *Deep Sea Res.*, *45*, 15–38.

Pacanowski, R., and S. G. H. Philander (1981), Parameterization of Vertical Mixing in Numerical Models of Tropical Oceans, *J. Phys. Oceanogr.*, *11*(11), 1443–1451.

Pickart, R. S. (2004), Shelfbreak circulation in the Alaskan Beaufort Sea: Mean structure and variability, *J. Geophys. Res.*, *109*, C04024, doi:10.1029/2003JC001912.

Polyakov, I. V., et al. (2005), One more step toward a warmer Arctic, *Geophys. Res. Lett.*, *32*, L17605, doi:10.1029/2005GL023740.

Prange, M., and G. Lohmann (2001), Variable freshwater input to the Arctic Ocean during the Holocene: Implications for large-scale ocean-sea ice dynamics as simulated by a circulation model, in *The KIHZ Project: Towards a Synthesis of Holocene Proxy Data and Climate Models*, edited by H. Fischer et al., Springer, New York.

Proshutinsky, A., et al. (2001), Multinational effort studies differences among Arctic Ocean models, *Eos Trans. AGU*, *82*(51), 637–644.

Proshutinsky, A., R. H. Bourke, and F. A. McLaughlin (2002), The role of the Beaufort Gyre in Arctic climate variability: Seasonal to decadal climate scales, *Geophys. Res. Lett.*, *29*(23), 2100, doi:10.1029/2002GL015847.

Proshutinsky, A., et al. (2005), Arctic Ocean study: Synthesis of model results and observations, *Eos Trans. AGU*, *86*(40), 368.

Röske, F. (2001), An atlas of surface fluxes based on the ECMWF re-analysis – a climatological data set to force global ocean general circulation models, *MPI Rep. 323*, Max-Planck-Inst. für Meteorol., Hamburg, Germany.

Rudels, B., E. P. Jones, L. G. Anderson, and G. Kattner (1994), On the intermediate depth waters of the Arctic Ocean, in *The Polar Oceans and Their Role in Shaping the Global Environment*, edited by O. M. Johannessen, R. D. Muench, and J. E. Overland, pp. 33–46, AGU, Washington, D. C.

Semtner, A. J., Jr. (1986), Finite-difference formulation of a world ocean model, in *Proceedings of NATO Advanced Physical Oceanographic Numerical Modeling*, edited by J. O'Brien, pp. 187–202, Springer, New York.

Smith, R. D., J. K. Dukowicz, and R. C. Malone (1992), Parallel Ocean General Circulation Modeling, *Physica D*, *60*, 38–61.

Steele, M., and T. Boyd (1998), Retreat of the cold halocline layer in the Arctic Ocean, *J. Geophys. Res.*, *103*, 10,419–10,435.

Steele, M., and W. Ermold (2007), Steric sea level change in the Northern Seas, *J. Clim.*, in press.

Steele, M., R. Morley, and W. Ermold (2001a), PHC: A global ocean hydrography with a high quality Arctic Ocean, *J. Clim.*, *14*, 2079–2087.

Steele, M., W. Ermold, G. Holloway, S. Hakkinen, D. M. Holland, M. Karcher, F. Kauker, W. Maslowski, N. Steiner, and J. Zhang (2001b), Adrift in the Beaufort Grye: A model intercomparison, *Geophys. Res. Lett.*, *28*, 2835–2838.

Woodgate, R. A., K. Aagaard, R. D. Muench, J. Gunn, G. Björk, B. Rudels, A. T. Roach, and U. Schauer (2001), The Arctic Ocean Boundary Current along the Eurasian slope and the adjacent Lomonosov Ridge: Water mass properties, transports and transformations from moored instruments, *Deep Sea Res., Part I*, *48*(8), 1757–1792.

Yang, J. (2005), The Arctic and subarctic ocean flux of potential vorticity and the Arctic Ocean circulation, *J. Phys. Oceanogr.*, *35*, 2387–2407.

Zhang, J., and W. D. Hibler III (1997), On an efficient numerical method for modeling sea ice dynamics, *J. Geophys. Res.*, *102*, 8691–8702.

Zhang, J., and D. A. Rothrock (2003), Modeling global sea ice with a thickness and enthalpy distribution model in generalized curvilinear coordinates, *Mon. Weather Rev.*, *131*(5), 681–697.

Zhang, J., D. A. Rothrock, and M. Steele (1998a), Warming of the Arctic Ocean by a strengthened Atlantic inflow: Model results, *Geophys. Res. Lett.*, *25*, 1745–1748.

Zhang, J., W. D. Hibler III, M. Steele, and D. A. Rothrock (1998b), Arctic ice-ocean modeling with and without climate restoring, *J. Phys. Oceanogr.*, *28*, 191–217.

Zhang, J., M. Steele, D. A. Rothrock, and R. W. Lindsay (2004), Increasing exchanges at Greenland-Scotland Ridge and their links with the North Atlantic Oscillation and Arctic sea ice, *Geophys. Res. Lett.*, *31*, L09307, doi:10.1029/2003GL019304.

M. Steele and J. Zhang, Polar Science Center, Applied Physics Laboratory, College of Ocean and Fishery Sciences, University of Washington, Seattle, WA 98105, USA. (zhang@apl.washington.edu)